13th International Symposium on Particle Image Velocimetry – ISPIV 2019
Munich, Germany, July 22-24, 2019

Transitional flow in a 90° pipe bend

Johannes Burkert[1]*, Rüdiger Schwarze[1], Katrin Bauer[1]

[1] TU Bergakademie Freiberg, Institute of Mechanics and Fluid Dynamics/Fluid Dynamics and Turbomachinery, Freiberg, Germany

* johannes.burkert@imfd.tu-freiberg.de

Abstract

The transitional flow in pipe bend flows has not been well explored in contrast to transitional flow in straight pipes. During the last decade the interest in understanding the flow development in pipe bends for different Reynolds numbers Re has increased. In order to fill the gap especially for flow transition, a new test rig which covers a range of $500 < Re < 7000$ has been designed and manufactured. Initial high speed particle image velocimetry (PIV) measurements were carried out in order to test the new set-up and to characterize the evolving flow structures in the relevant Reynolds number range. For this purpose the measurements were concentrated on the stream wise flow of the bend and upstream the bends outlet region. The results show that the test rig is operating and that it does not distort the flow development.

1 Introduction

Transitional flow in a straight pipe has been well explored and understood up to date. Most importantly, Hof et al. (2004) observed nonlinear traveling waves denoting the onset of turbulent flow. Further work on the transition in pipe flow was done by Eckhardt et al. (2007) and Van Doorne and Westerweel (2007) who determine the transition process as a mostly chaotic process which is dominated by nonlinear traveling waves. During transition hairpin like structures grow up and become big vortex areas. The onset of this process is not periodically what is characteristic for the transition from laminar to turbulent flow.

However, the transitional behavior of flow in pipe bends is still not fully understood. It is known that at above a critical value of the Dean number ($De > 10$) the so called Dean vortices develop as a pair of secondary vortices Dean (1927); Fresconi and Prasad (2007). For higher Reynolds numbers (Re = 50000 - 200000) in the fully turbulent flow regime, Tunstall and Harvey (1968) first found additional swirl superposed to the Dean vortices downstream the pipe bend. The swirl orientation changes periodically and is referred to as swirl switching, probably caused by flow separation (Tunstall and Harvey (1968)). Thirty years later, Brücker (1998) observed a characteristic frequency for the swirl switching which identifies this phenomenon as a combination of low and high frequency flow structures. Recent studies e.g. by Hufnagel et al. (2017) in a similar Reynolds number-range confirmed these characteristic frequencies found by Brücker (1998). The origin of the swirl switching is supposed directly in the bend itself and may be caused by shear layer instabilities (Rütten et al. (2005)). Moreover, the phenomenon is not a movement of the Dean cells but a change between two distinct states. In other words, one Dean cell is suppressing the other cell in a periodic manner (Rütten et al. (2005)). Kalpakli et al. (2010); Kalpakli and Örlü (2013); Kalpakli et al. (2015, 2016) together with Carlsson et al. (2015) have done several experimental as well numerical work on the swirl switching process for different Reynolds numbers. They found the same range of frequencies to be an identification for the swirl switching and that the curvature ratio has the most impact besides the Reynolds number on the switching intensity. Noorani and Schlatter (2016) found the swirl switching process in a closed toroidal pipe, too.

However, up to date the onset or rather the responsible structures of swirl switching has not been fully understood. Moreover, the development of characteristic flow in 90° pipe bends during laminar-turbulent transition has to the best of our knowledge not been investigated experimentally, yet.

2 Experimental Setup

In order to fill this gap a new test rig has been built to cover the range of $1000 < Re < 6000$ in bend pipe flow. The main idea of the test rig (Fig. 1(a)) is to measure the flow structure in simple planar PIV, as well as stereo PIV, up to fully three-dimensional flow without optical distortions. Thus, the pipe's (D = 30 mm) material is silicone (refractive index n = 1.4095) surrounded by an octagonally shaped housing made from Plexiglas for optical access from all side walls. The entrance length before the bend is L = 30 D to ensure fully developed flow conditions. The flow rate is adjustable by a drive controlled centrifugal pump. The pump set up allows, in combination with a bypass, Reynolds numbers of 500 up to 7000. The refractive index of the silicone is matched by the use of a water/glycerin mixture (48 % to 52 %, $\nu = 8.4 \times 10^{-6}\,\mathrm{m^2\,s^{-1}}$. The hydraulic scheme of the test rig is displayed in Fig. 1(b). The following characteristic numbers apply for the experiments and

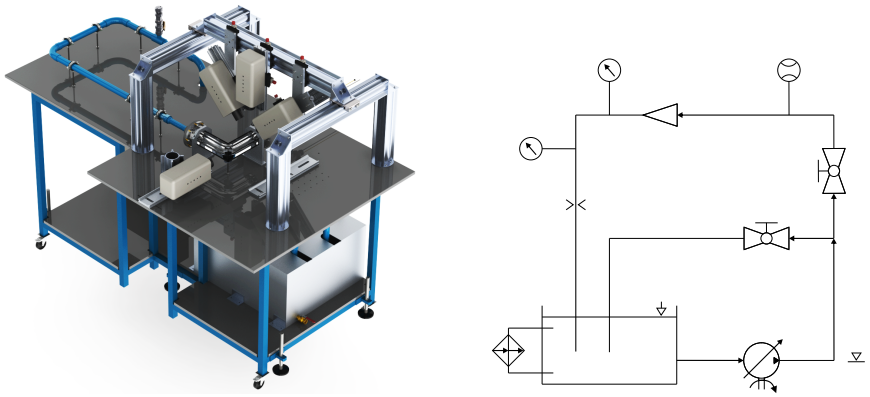

(a) (b)

Figure 1: a) CAD Rendering of the experimental setup and b) hydraulic scheme of the test rig.

later on for the evaluation of the results. The Reynolds number *Re* is based on the pipe diameter D, the bulk velocity u_0 and the kinematic viscosity ν of the fluid. The Strouhal number *Str* is determined with the characteristic frequency f, D and u_0 and is needed to compare the power spectrum of the flow structures (see section 6). The bulk velocity u_0 is received from the flow rate $\dot{V}$ and the cross-sectional area of the pipe.

$$Re = \frac{D\,u_0}{\nu} \qquad Str = \frac{f\,D}{u_0} \qquad u_0 = \frac{4}{\pi}\frac{\dot{V}}{D^2} \tag{1}$$

2.1 PIV Mesaurements

Initially, planar high-speed measurements were carried out at the pipe bend to get first impressions of the transitional flow structures. The optical set-up for the flow measurements is shown in Fig. 2 and 3 for two different measurements planes. The experiments were performed by using a single cavity high-speed laser (*Litron Nd:YLF LDY 300/350 Series*) synchronized with a high-speed camera (*Phantom V12*, window size 1280 x 800 pixels, pixelsize 20 µm). The camera was equipped with a macro-lens (*Tokina* 90 mm, 1:2.8, f5.6) for the top-view measurements and a 50 mm lens (*Nikon* AF 50 mm f/1.8D) for the recording of the inlet flow. The fluid was seeded with *Vestosint* tracer-particles (density 1060 $\mathrm{kg\,m^{-3}}$, $d_p \approx 50$ µm).

The Reynolds number was varied between 2000 and 6000 with recording frequencies in the range of 1200 Hz up to 4000 Hz. The first measurement plane was chosen to observe the stream wise flow before the bend inlet (Fig. 2). Whith the second set-up we observe the flow downstream the pipe bend with a top-view (3). Both measurements are performed to characterize the test rig with respect to the specific frequencies of certain flow structures like the Dean vortices and the corresponding swirl switching. A number of 2500 images are recorded for every Reynolds number. The inlet flow conditions are investigated to get an impression of the incoming flow profile and possible instabilities. The light sheet position ranged from 4D to 1.5D upstream the bend inlet.

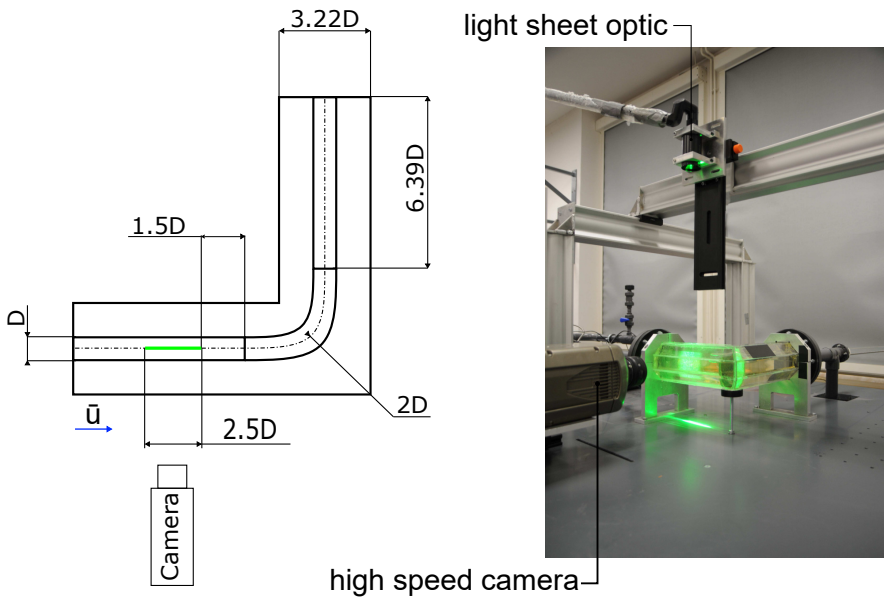

Figure 2: Experimental setup for the planar PIV mesaurements upstream the bend inlet. All sizes are related to the pipe diameter D.

The second measurement shall provide an impression of the development of secondary flow structures from a top-view position. The light sheet is placed at the bend's symmetry plane so that the flow is visible from the half of the bend region up to 3.22 D_{max} downstream the bend. To compare the results from both set-ups the Reynolds numbers are the same for each record.

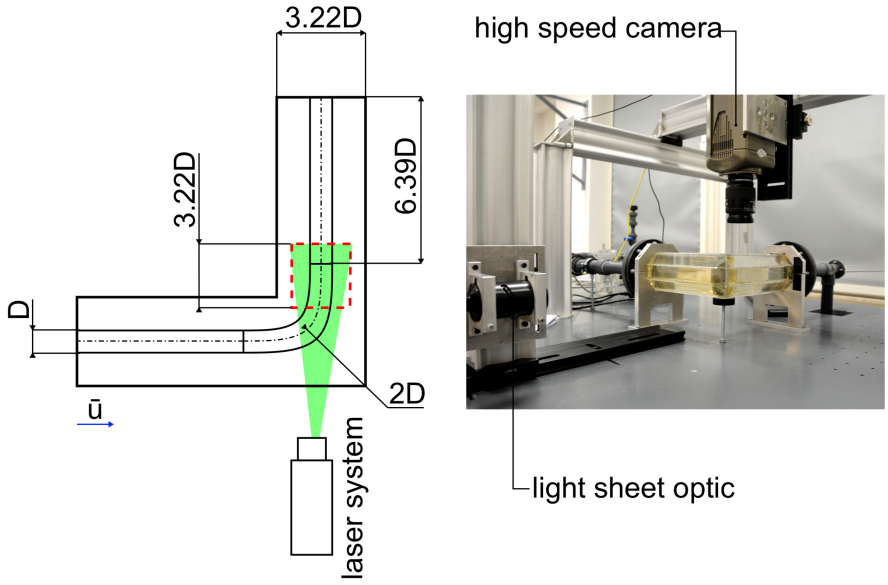

Figure 3: Experimental set-up for the top-view measurements on the bends outlet region. All sizes are related to the pipe diameter D.

2.2 Methods

The obtained raw images are analyzed in *DaVis 8, LaVision* to create the velocity vector fields based on a 2D cross correlation method. The calculation was done in two correlation passes with first 32 x 32 pixels window size and a second pass with 12 x 12 pixels with an window overlap of 50 %. Further post-processing

(color-plots, vector-plots and fast fourier transformation) was done in *Matlab2018*. To calculate the frequencies of the characteristic flow structures a fast fourier transformation (FFT) was performed. According to Hufnagel et al. (2017) a 3D proper orthogonal decomposition (POD) is the best method to obtain an accurate result of the FFT. But in case of a 2D planar PIV, the POD method is inapplicable because of the missing third velocity component (Wang et al. (2018)). Thus, the velocity signal at a line source at five different positions downstream the bend was used as the input for the FFT (Fig. 5). Data evaluation based on point sources strongly depends on the chosen location of the point (Wang et al. (2018)). Hence, the spatial velocity mean value was calculated at every single line to overcome this problem.

3 Results and Discussion

The results of the first measurement can be seen in Fig. 4 as color-pots with vector-arrows of the mean velocity field. It is obvious from the top pictures that the flow is uniform and fully developed when entering the bend. However, considering the temporal averaged development of the flow, clear instabilities are visible even for $Re = 2000$. We indicated this as first instabilities for the transition from laminar to turbulent flow. As described by Hof et al. (2004) and Van Doorne and Westerweel (2007) there are several puff and slug like structures which can be estimated from the velocity field. Fig. 4 shows the mean velocity field (top images) and instantaneous velcity and vector fields for different time-steps t_0, t_1 and t_2 ($\Delta t = 0.09\,\mathrm{s}$ for $Re = 2000$, $\Delta t = 0.03\,\mathrm{s}$ for $Re = 6000$) as an example for the temporal development of the flow before it enters the pipe bend. The red dashed circles indicate the onset of quasi-periodic structures which are deduced as puffs or slug like structures. For $Re = 2000$ these structures are much more pronounced than for $Re = 6000$ where only small patterns can be seen on the sub-sequential color-maps.

The results of the top-view measurement are presented in the following passage. Fig. 5 shows exemplary the velocity contour plots for $Re = 2000$ (left side) and $Re = 6000$ (right side) directly in the bend (top view). At the top of the figure the mean velocity field is displayed likewise instantaneous snapshots are presented below. The time-step among the pictures is 0.17 s for the laminar and 0.03 second for the turbulent case. The different time-steps for $Re = 2000$ arise from the slowly appearance of the flow structures. It is visible that the flow is separated into two regions. One primary uniform region of high-speed flow occurs at the outer radius of the pipe bend and a secondary high-speed region can be identified near the inner radius of the pipe bend. Both regions are marked by the blue dotted line in Fig. 5 and are numbered with 1 (outer region) and two (inner region). The onset of the secondary high-speed region differs between the Reynolds numbers. For $Re = 2000$ this start point is at $x/D \approx -0.1$ whereas for $Re = 6000$ it occurs already at $x/D \approx -0.25$, but is much less pronounced. Furthermore, the thickness of the primary high speed region at the outer wall differs between the two investigated Reynolds-numbers with a higher thickness for larger Re. Moreover, the time resolved measurements reveal the secondary high speed region to become already unstable for a Reynolds numbers of $Re = 2000$. In other words, there is a periodic built up of the secondary high speed region, which pushes fluid downstream the pipe. This might be related to the swirl switching. This periodic behavior is indicated by the red dashed line in Fig. 5. The origin of the second high speed region 'moves' in between -0.35 D and 0.0 D for $Re = 2000$ and -0.2 D and -0.1 D for $Re = 6000$.

Next, the results of the FFT are discussed and displayed in Fig. 6. The results were normalized to the maximum value of the power spectral density (PSD) for better comparability and were made dimensionless using the Strouhal number. The results reveal distinct peaks at $Str = 0.005$ and $Str = 0.2 \cdots 0.4$ for $Re = 2000$ and $Str = 0.005$ and more peaks at $Str = 0.15 \cdots 0.3$ and in between $Str = 0.4 \cdots 0.6$ for $Re = 6000$. According to Hellström et al. (2013), the low frequency indicates the motion of the two Dean cells while larger frequencies represent the swirl switching or other turbulent structures like vortices. It is conspicuous that even for $Re = 2000$ the transition already sets in. To prove the practicality of the spatial velocity mean value five different locations for the line was chosen. The positions are represented in Fig. 5 on the top by the black dashed lines.

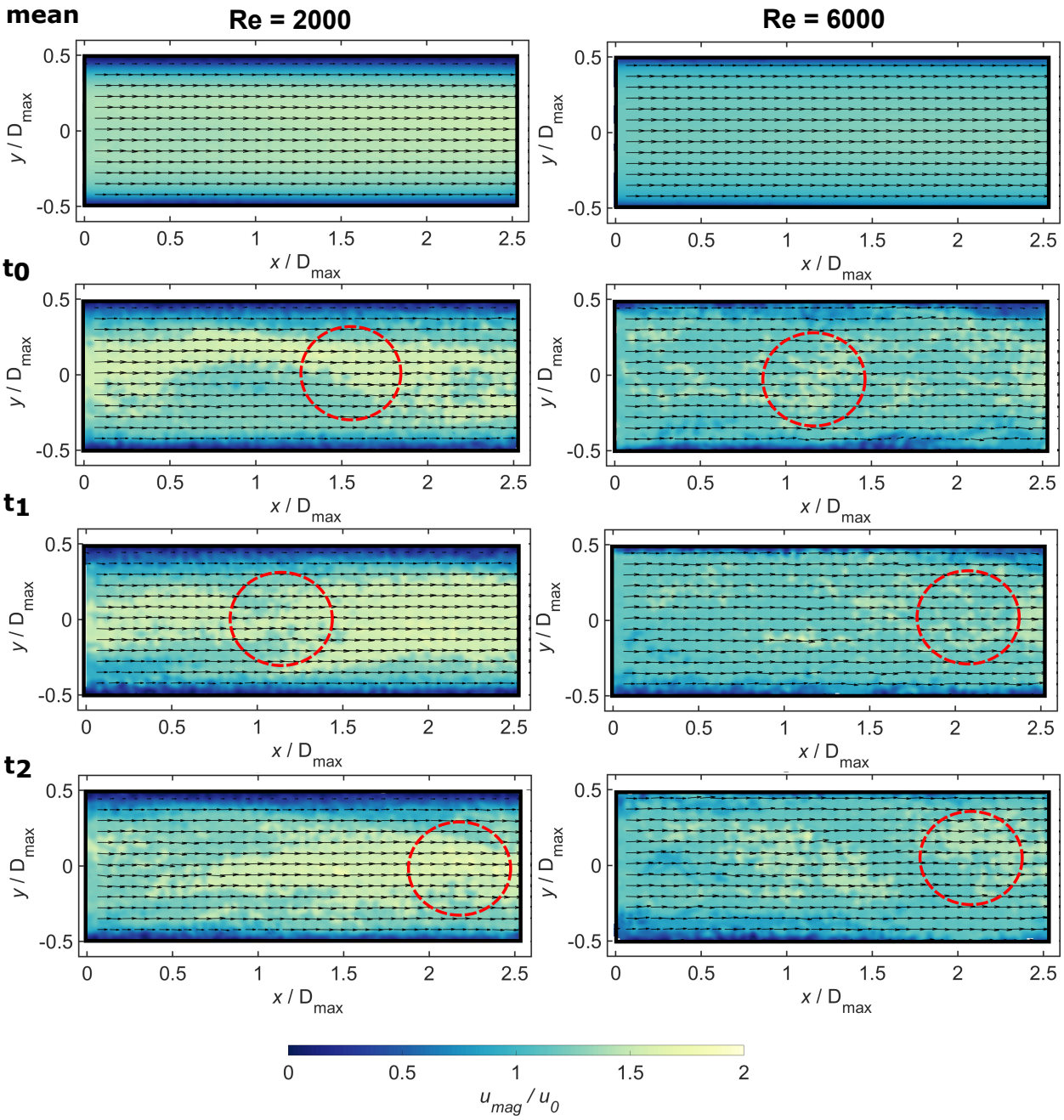

Figure 4: Results of the planar PIV for $Re = 2000$ (left side) and $Re = 6000$ (right side) at a plane ranged from 4D to 1.5D upstream the bend inlet (presented as 0D to 2.5D). The velocity mean values are displayed at the top and instantaneous velocity color-maps (at subsequent time steps) are plotted below. The fluid is moving from the left to the right side.

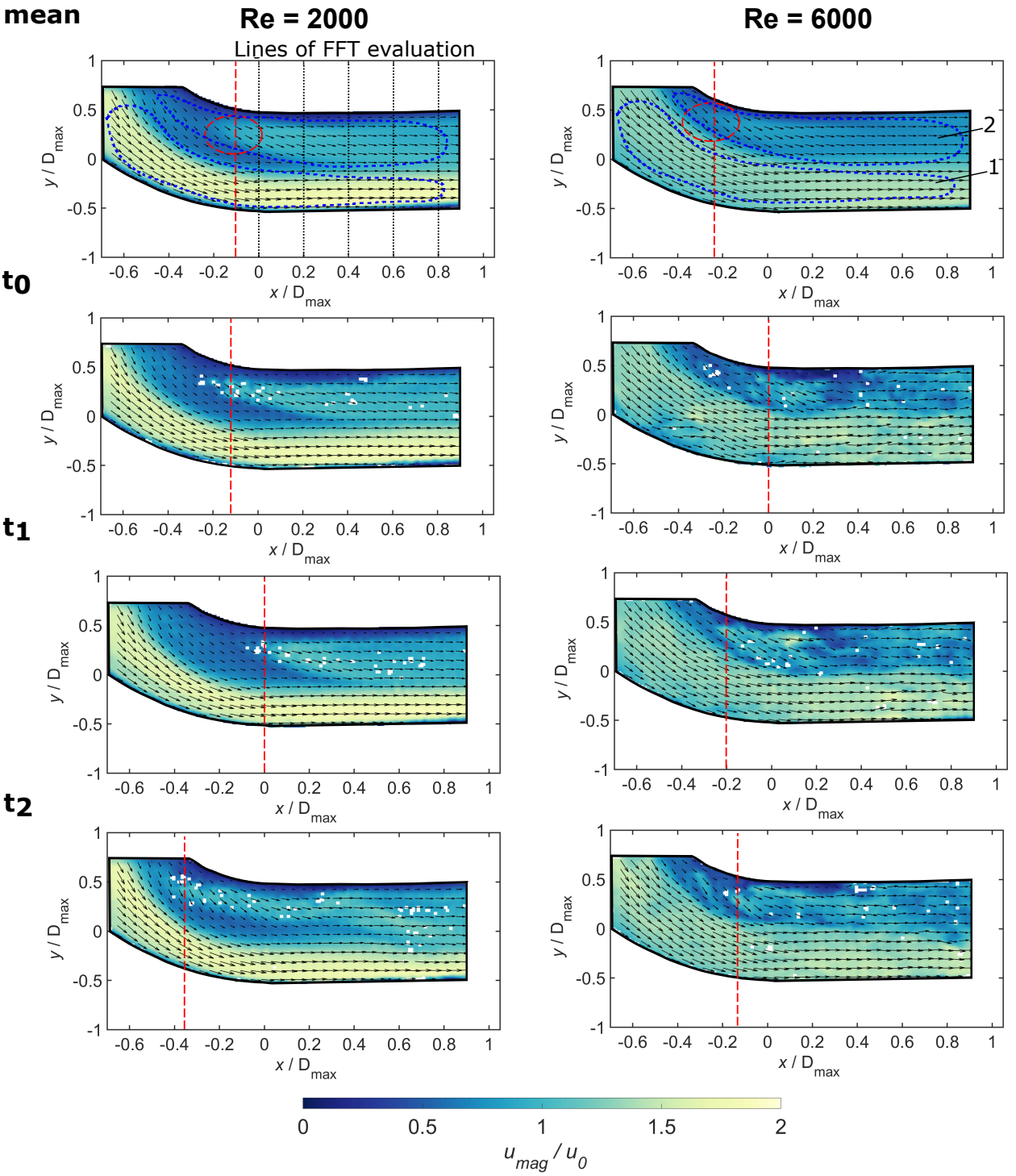

Figure 5: Results of topview planar PIV for $Re = 2000$ (left side) and $Re = 6000$ (right side). Velocity mean values are displayed at the top and instantaneous velocity fields at different times are presented below. The red dashed line indicates the movement of the origin region of the inner high speed region.

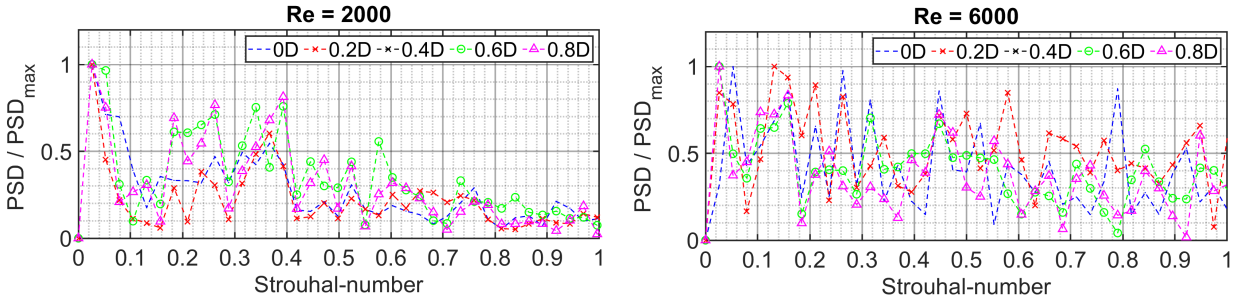

(a) (b)

Figure 6: Results of the FFT for a) $Re = 2000$ and b) $Re = 6000$ at five different positions at the bend's outlet.

4 Conclusion

Our measurements demonstrate that the chosen experimental setup and the applied methods to calculate the frequency spectrum are suitable to examine the flow during transition. The results match with previous works regarding the observed flow structures and associated frequencies, as well. Also, we could define a range of Reynolds numbers from interest for later measurement mean by time resolved planar, stereo and 3D PIV at different regions of the pipe bend to better understand the swirl switching as well the transition process itself. Especially the time resolved measurements show that local transition processes seems to set in already at $Re = 2000$ due to the fluids acceleration at the outer and deceleration at the inner pipe diameter. For both investigated Reynolds numbers, a periodic onset of the inner high speed region was observed. The mechanism driving these fluctuation is not yet clear. Based on these findings, further investigations by means of time resolved planar, stereo PIV and 3D PTV measurements will be done on the basis of the initial experiments.

References

Brücker C (1998) A Time-Recording Dpiv-Study of the Swirl Switching Effect in a 90 Bend Flow. *Proc 8th International Symposium on Flow Visualization, Sorrento(NA), Italy* pages 171.1–171.6

Carlsson C, Alenius E, and Fuchs L (2015) Swirl switching in turbulent flow through 90 pipe bends. *Physics of Fluids* 27

Dean W (1927) Note on the motion of fluid in a curved pipe. *The London, Edinburgh, and Dublin Philosophical Magazine and Journal of Science* 4:208–223

Eckhardt B, Schneider TM, Hof B, and Westerweel J (2007) Turbulence Transition in Pipe Flow. *Annual Review of Fluid Mechanics* 39:447–468

Fresconi FE and Prasad AK (2007) Secondary velocity fields in the conducting airways of the human lung. *Journal of Biomechanical Engineering* 129:722–732

Hellström LHO, Zlatinov MB, Cao G, and Smits AJ (2013) Turbulent pipe flow downstream of a 90 bend. *Journal of Fluid Mechanics* 735:R7

Hof B, van Doorne CWH, Westerveel J, Nieuwstadt FTM, Faisst H, Eckhardt B, Wedin H, Kerswell RR, and Waleffe F (2004) Experimental Observation of Nonlinear Traveling Waves in Turbulent Pipe Flow. *Science* 305:1594–1598

Hufnagel L, Canton J, Oerlue R, Marin O, Merzari E, and Schlatter P (2017) The three-dimensional structure of swirl-switching in bent pipe flow. *Journal of Fluid Mechanics* 835:86–101

Kalpakli, Örlü Ramis, Tillmark Nils, and Alfredsson P Henrik (2010) Experimental Investigation on the effect of pulsations on turbulent flow through a 90 degrees pipe bend. *Int Conf on Jets,Wakes and Separated Flows* pages 1–6

Kalpakli A and Örlü R (2013) Turbulent pipe flow downstream a 90 pipe bend with and without superimposed swirl. *International Journal of Heat and Fluid Flow* 41:103–111

Kalpakli A, Örlü R, and Alfredsson PH (2015) POD analysis of the turbulent flow downstream a mild and sharp bend. *Experiments in Fluids* 56

Kalpakli A, Sattarzadeh SS, and Örlü R (2016) Combined hot-wire and PIV measurements of a swirling turbulent flow at the exit of a 90 pipe bend. *Journal of Visualization* 19:261–273

Noorani A and Schlatter P (2016) Swirl-switching phenomenon in turbulent flow through toroidal pipes. *International Journal of Heat and Fluid Flow* 61:108–116

Rütten F, Schröder W, and Meinke M (2005) Large-eddy simulation of low frequency oscillations of the Dean vortices in turbulent pipe bend flows. *Physics of Fluids* 17

Tunstall MJ and Harvey JK (1968) On the effect of a sharp bend in a fully developed turbulent pipe-flow. *Journal of Fluid Mechanics* 34:595–608

Van Doorne CW and Westerweel J (2007) Measurement of laminar, transitional and turbulent pipe flow using Stereoscopic-PIV. *Experiments in Fluids* 42:259–279

Wang Z, Örlu R, Schlatter P, and Chung YM (2018) Direct Numerical Simulation of Turbulent Pipe Flow. *International Journal of Heat and Fluid Flow* 73:100 – 208